Grzegorz Michta, Aleksandra Wilk

Laser-Welded Joints Made of Steels 304L and 904L Used in the Automotive Industry

Abstract: The article presents results of tests concerning welded joints made of alloy steels AISI 304L and AISI 904L using a high-power Nd:YAG laser. Tests involving the joints and aimed to identify their mechanical properties included tensile tests and microhardness measurements. The research work discussed in the article also involved the performance of microstructural tests of the base materials and welds as well as fractographic examinations.

Keywords: steel 304L, steel 904L, laser welding, automotive industry, microstructure, mechanical properties

DOI: 10.17729/ebis.2023.4/3

Introduction

Presently, laser beam welding is one of the methods most common used in the joining of metallic materials. The laser beam, which belongs to highly-concentrated heat sources applied in welding processes, is characterised by the high parallelism and density of energy as well as by low energy scatter. As a result, the laser beam welding process enables the obtainment of the small heat affected zone (HAZ) of the material subjected to processing as well as the small amount of material melted in the welding area. Laser can be used in the welding of most metals and their alloys as well as plastics [1].

Because of the presence of alloying agents and their contents, the weldability of alloy steels depends on a larger number of factors than that of unalloyed steels. Because of this, the welding process should be performed so that the formation of welding imperfections in the welded joint could be prevented and that the weld as well as the HAZ could satisfy requirements concerning steel structures [2].

Steels AISI 304L and AISI 904L belong to the group of stainless steels or, more precisely, austenitic stainless steels. Steel AISI 304L is a popular steel grade commonly used in industry and available on the market. The steel is characterised by high corrosion resistance as well as excellent formability and weldability. In addition, steel AISI 304L is one of the cheapest stainless steels grades available [1]. In turn, high-alloy austenitic steel AISI 904L is best-known for the high stability of its austenitic phase and high corrosion resistance. Because of high contents of alloying elements, the steel is used where very high corrosion resistance is required and the cost of application does not constitute a key aspect [3].

Tests concerning the laser beam welding of steels AISI 304L and AISI 904L discussed in this article aimed to preliminarily assess the possibility of making joints using a robotic welding station (primarily in relation to the precise fixing of small-thickness unprocessed sheets). The abovenamed materials are used, among other things, in the fabrication of plate heat exchangers. An attempt at joining steel AISI 904L with AISI 304L was dictated by the high cost of the former and in order to limit its use to the zone of gas condensation, i.e. the area which should be characterised by higher corrosion resistance.

Materials and testing methodology

The element subjected to the tests was a solid-state laser welded joint (method 521) made of 1.5 mm thick steel AISI 304L and AISI 904L (Fig. 1). The designation of steel AISI 304L in accordance with the PN-EN 10088-1 standard is X5CrNi18-10 (1.4307), whereas that of steel AISI 904L in

dr inż. Grzegorz Michta, Akademia Górniczo-Hutnicza im. Stanisława Staszica w Krakowie (AGH University of Science and Technology in Kraków)

mgr inż. Aleksandra Wilk, Pratt & Whitney, Rzeszów

Table 1. Chemical composition of steel AISI 304L and AISI 904L [4]

Material	C	Si	Mn	P	S	N	Cr	Cu	Mo	Ni
1.4307	0,03	1,00	2,00	0,045	0,015	0,11	17,5–19,5	–	–	8,00–10,5
1.4539	0,02	0,70	2,00	0,030	0,010	0,15	19,0–21,0	1,2–2,0	4,0–4,5	24,0–26

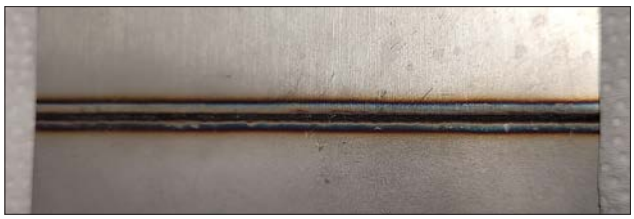

Fig. 1. Laser beam welded joint (method 521) made of steels 304L and 904L

accordance with the PN-EN 10088-1 standard is X1NiCrMoCu25-20 -5 (1.4539). The chemical compositions of both steel grades are presented in Table 1 [4].

The welding process involved the use of 1.5 mm thick water jet-cut sheets which were previously cleaned using isopropyl alcohol (IPA) cleaning, stiffened and joined using laser tack welds.

The test welded joints were made using an HPFL Nd:YAG IPG YLS 3000 – CT – Y15 laser source, where HPFL stands for a high power fibre laser, Nd:YAG stands for a solid-state laser emitting the laser beam in a pulsed mode, IPG is the name of the company producing the most technologically advanced laser power sources, YLS stands for an ytterbium laser system and 3000 represents the nominal power of the source. The producer's designation of the laser power source is IPG YLS 3000 – CT – Y15. The beam was focused by a lens-collimator system (F120/F250). The focal length amounted to 159 mm, the laser beam focus diameter amounted to 376 μm and the laser probe angle of inclination amounted to 0°; the beam struck the material perpendicularly. The laser beam welding process was performed using a power of 820 W, a welding rate of 1000 mm/min as well as a shielding gas (Ar) flow rate of 30 l/min (used to protect weld face) and that of 5 l/min (used to protect the weld root). The shielding gas nozzle was located 2 mm away from (behind) the focus and directed towards the weld pool.

The materials used in the metallographic tests were sampled so that the process of cutting would not trigger changes in the microstructure (by adjusting the proper rate of cutting and that of coolant feeding). Metallographic specimens (both in the etched and unetched state) were subjected to microscopic tests. The electrolytic etching process was performed using the 10% aqueous solution of CrO_3.

The microstructural tests were performed using the following microscopes and imaging techniques:

- Axio Imager M1m light microscope (LM) (ZEISS); bright visual field and Nomarski interference contrast (NIC),
- Merlin Gemini II scanning electron microscope (SEM) (Zeiss) provided with EDS Quantax 800 and EBSD Quantax CrystAlign 400 microanalytical systems; secondary electron (SE) and back-scattered electron (BSE) imaging.

The microstructural tests involved the sampling of specimens from the cross-section of joints subjected to the tests. Specimens used in tensile tests were prepared in accordance with a related standard concerning destructive tests of welded joints related to the tensile tests of transverse specimens. [5]. Specimens used in the tests were flat. The performance of the static tensile tests was followed

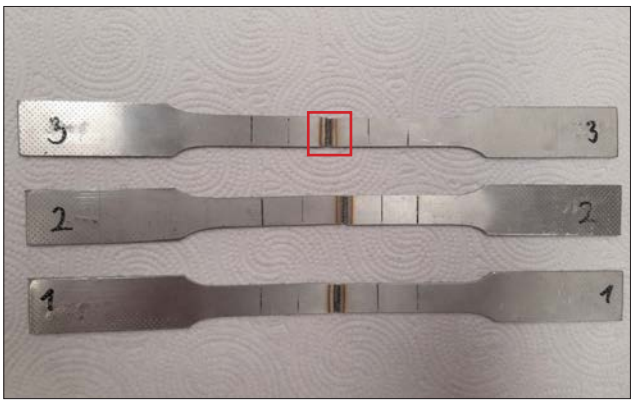

Fig. 2. Specimens after the static tensile tests

by measurements concerning the elongation of the specimens and the area of their reduction. The specimens after the tensile tests are presented in Figure 2.

The fractographic tests involved the fractures of specimen no. 3 (marked red in Figure 2). The tests, performed using scanning electron microscopy (SEM), aimed to present the location of the joint fracture in relation to the microstructure present in the cross-section of the joint. The specimen used in the scanning electron microscopy-based tests is presented in Figure 3.

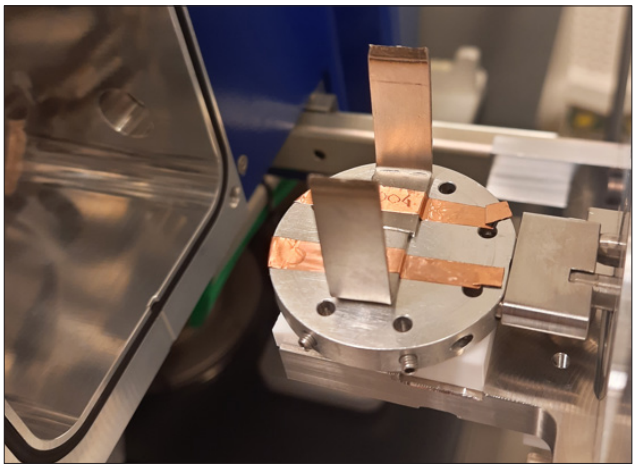

Fig. 3. Specimens fixed before scanning electron microscopic observations

The welded joints were also tested for the distribution of microhardness. The measurements involved the use of the Vickers hardness test, a load of 100 g and a load affecting time of 10 s.

Test results

Microstructural tests

The microstructure of the specimens was observed using a light microscope (LM) and a scanning electron microscope (SEM) (Figure 4). In both cases, austenitic grains were homogenous and contained twins (typical of the above-named steels), which confirmed that the microstructure of steel AISI 904L and that of steel AISI 304L were austenitic. The homogenous grains indicated that plastic processing was followed by recrystallisation, where austenite grains observed in steel AISI 904L were larger than those visible in steel AISI 304L.

Steel AISI 304 contained banded precipitates (resulting from plastic processing), where austenite grains were larger than the distance of precipitates present between the bands (which indicated that they did not affect the process of grain growth during recrystallisation). The identification of the precipitates involved the local EDS analysis of the

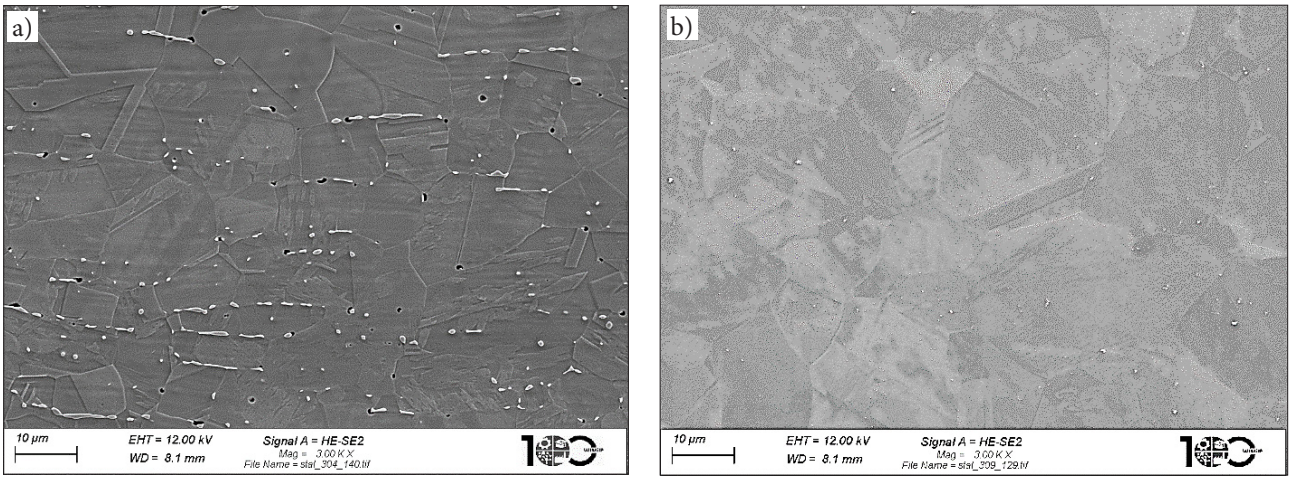

Fig. 4. Microstructure of the sheets used when making the test welded joints: a) steel AISI 316L and b) steel AISI 904L; metallographic specimen subjected to etching, SEM

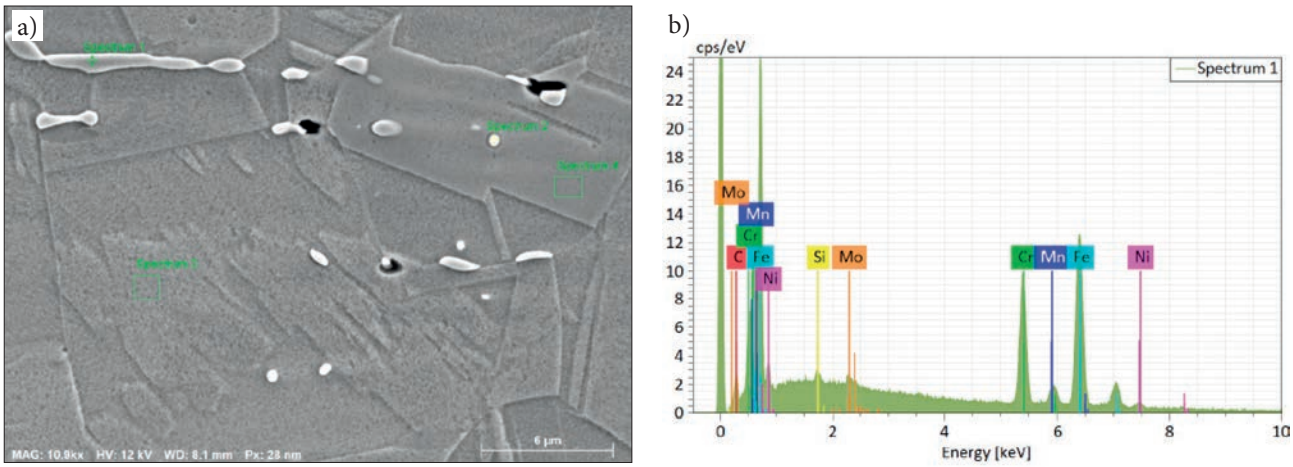

Fig. 5. Microstructure of steel AISI 304L (SEM): a) banded arrangement of carbides against the background of austenite grains with the area subjected to local EDS analysis and b) SEM EDS-based analysis of the chemical composition of a selected area

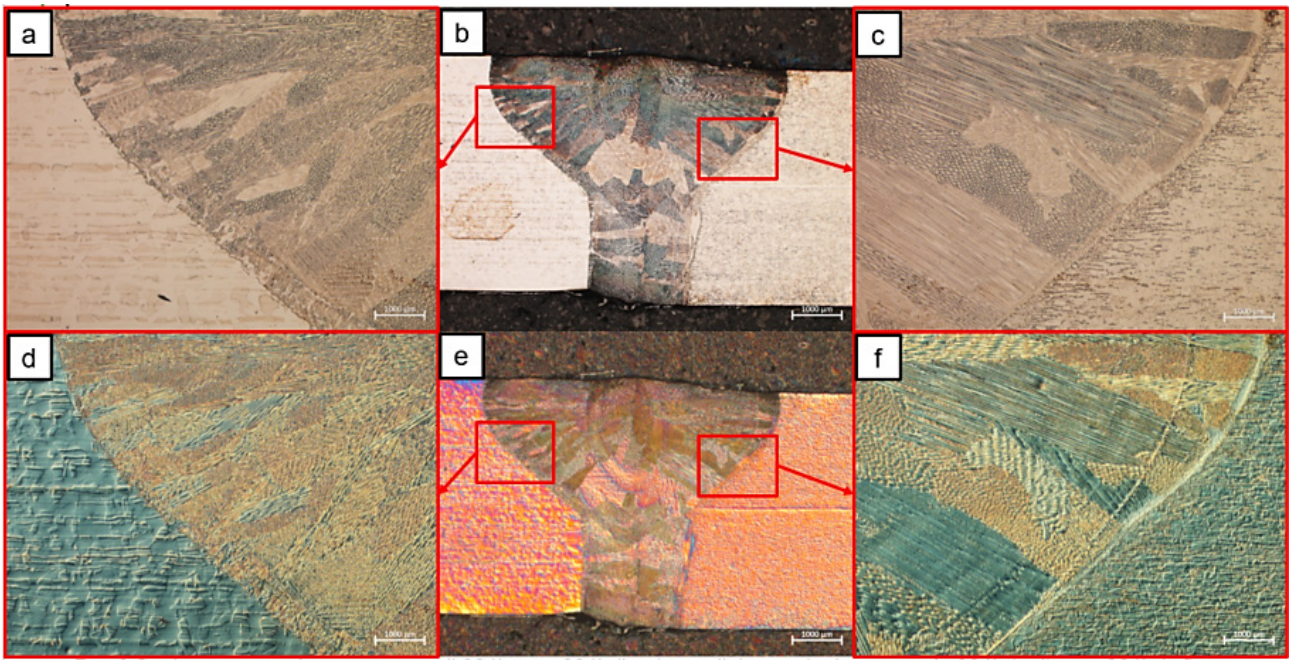

Fig. 6. Microstructures of the welded joints: a) and d) observed from the side of steel 304L; c) and f) observed from the side of steel 904L; light microscope, a), b) and c) bright visual field and d), e) and f) Nomarski interference contrast

chemical composition (Fig. 5). The area subjected to analysis is presented in Figure 5a (item 1 indicated with the arrow).

The examination of the chemical composition of the banded precipitate revealed the presence of chromium and molybdenum, where the remaining chemical elements observed in Figure 5b originated from the matrix. The foregoing was implied by the type of the carbide containing these elements, i.e. $(CrMo)_{23}C_6$, yet only diffraction tests could provide a definitive answer.

Figures 6 and 8 present the entire-cross section of the welded joint with its characteristic areas, i.e. the weld, the fusion line and the base material.

Figures 6b and 6e present the cross-section of the welded joint. It was possible to observe that the weld face was significantly larger than the weld root. Such a situation resulted directly from the application of the welding technology and the adjustment of welding parameters. The application of the Nomarski interference contrast technique made it possible to clearly observe the fusion line as well as the microstructure of the weld and that of the base material.Figure 7 presents the weld microstructure characterised by the presence of relatively large areas containing crystallites having the same crystallographic structure.

Figure 8 presents the microstructure of the welded joint observed using the scanning electron microscope (SEM).

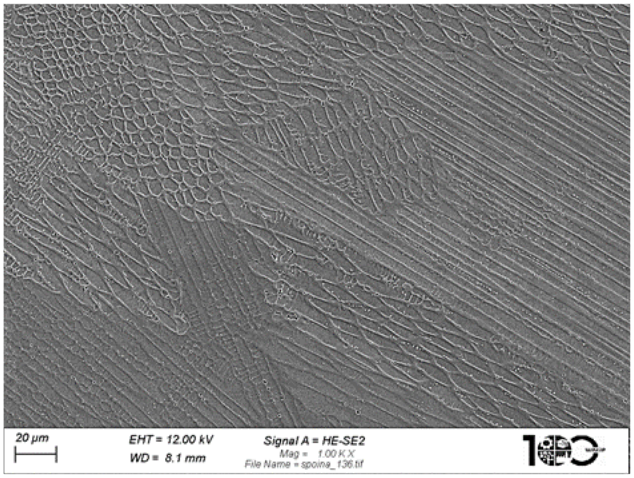

Fig. 7. Weld microstructure; etched metallographic specimen; SEM

The SEM-based observations confirmed observations performed using the light microscope. The base material was composed of homogenously arranged austenite grains, where the grains of steel AISI 904L were larger than those of steel AISI 304L. The precipitates observed in steel AISI 304L were arranged in the banded-like manner, which indicated the significant extent of steel processing. The SEM-based observations revealed the presence of small HAZ areas in the sheets (Fig. 8a and 8c), which could be ascribed to the application of a highly-concentrated heat source (laser), the use of which entailed the occurrence of high cooling rates.

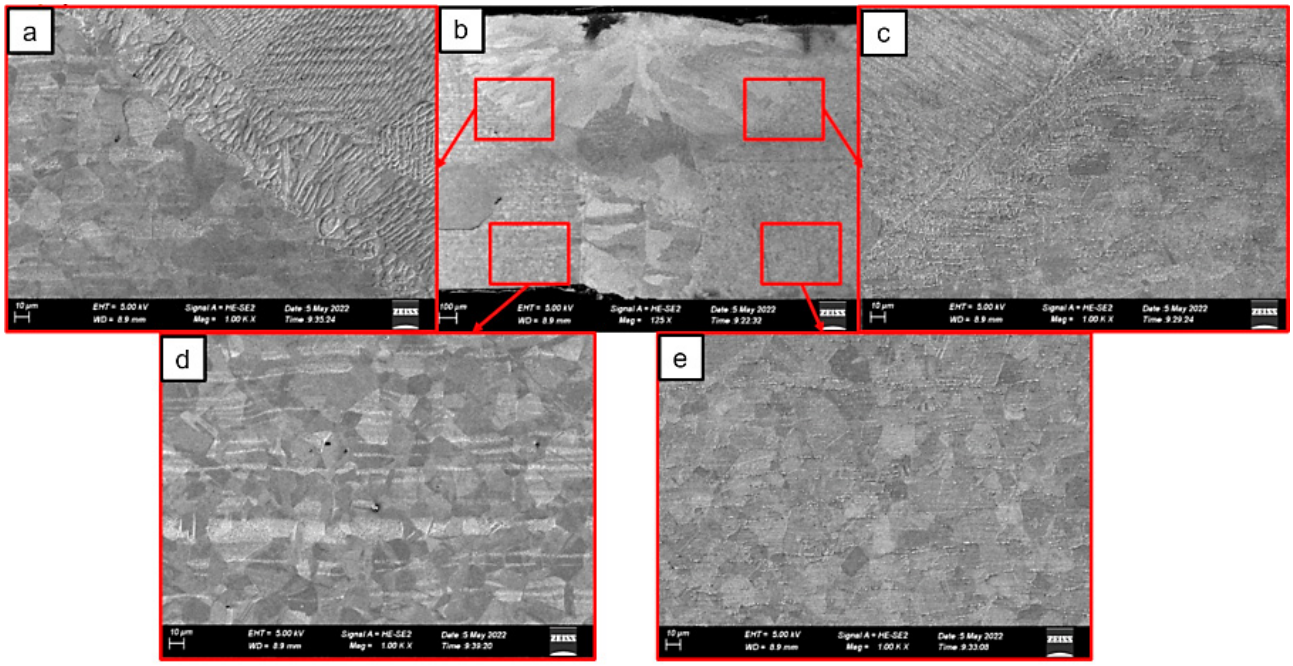

Fig. 8. Welded joint microstructure: a) and d) observed from the side of steel AISI 904L; c) and e) observed from the side of steel 304L, SEM

Static tensile tests

The static tensile tests were performed using an MTS 810 testing machine and three appropriately placed specimens. The specimens were prepared in accordance with the requirements specified in the PN EN ISO 4136 standard. Figure 9 presents stress-strain curves converted into stress in the function of strain. The average value of tensile strength amounted to 622 MPa (647.9 MPa, 606.1 MPa and 611.4 MPa), whereas that of strain amounted to 41%.

The observations of the fractures obtained in the tensile tests revealed that all the specimens ruptured in the weld. The macroscopic view of the welded joint is presented in Figure 10.

Fractographic tests revealed that fractures were most probably initiated in the weld axis and propagated towards steel AISI 904L, which could be attributed to its lower mechanical properties. The

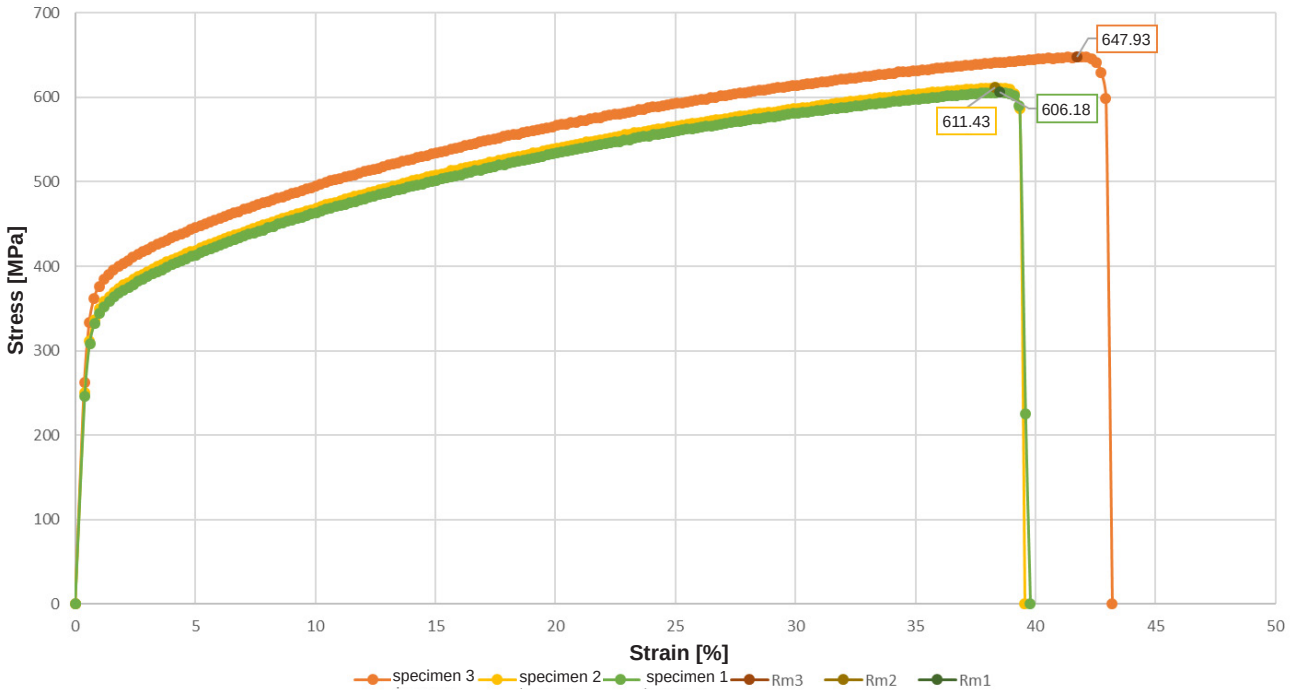

Fig. 9. Curves obtained in the static tensile tests of the welded joints made of steel AISI 304L and AISI 904L

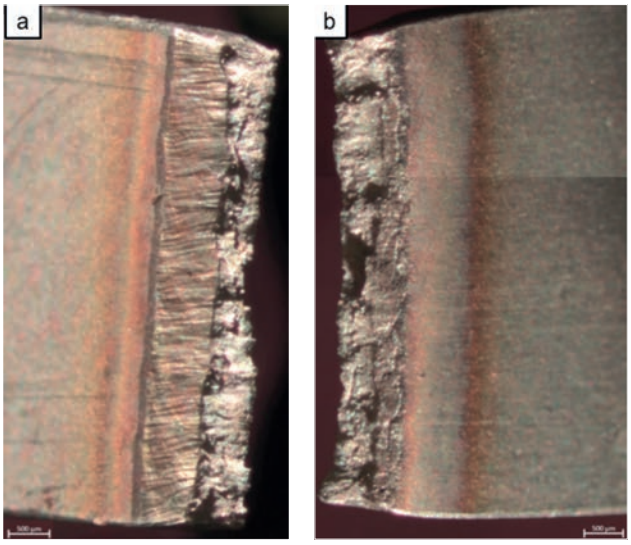

Fig. 10. Welded joint fractures: a) on the side of steel AISI 304L and b) on the side of steel AISI 904L

rupture was also characterised by area reduction triggered during the tensile test. The fractures were observed from the side of steel AISI 304L (Fig. 11) and steel AISI 904L (Fig. 12). The morphology of the fractures was tested using the scanning electron microscope (SEM).

Fractographic observations performed at low magnification (100×) revealed that the fracture surface was flat, which could imply its quasi-brittle or mixed nature. However, observations performed at greater magnification (5000× and 20000×) revealed the presence of characteristic pits, typical of plastic factures. Some of the pits contained precipitates.

Microhardness measurements

The size of the welded joint necessitated the performance of Vickers microhardness tests under a load of 0.9807 N. The tests were performed in two directions, i.e. longitudinal: base material (steel) AISI 904L – weld – base material (steel) AISI 304L (Fig. 13) and transverse: from the weld face to the weld root in the weld centre (Fig. 14).

The hardness distribution-related results revealed that steel AISI 304L was characterised by slightly higher hardness (224HV) than that of steel AISI 904L (187HV). In turn, the average hardness of the weld measured along the test joint amounted to 197HV, whereas that measured across the weld

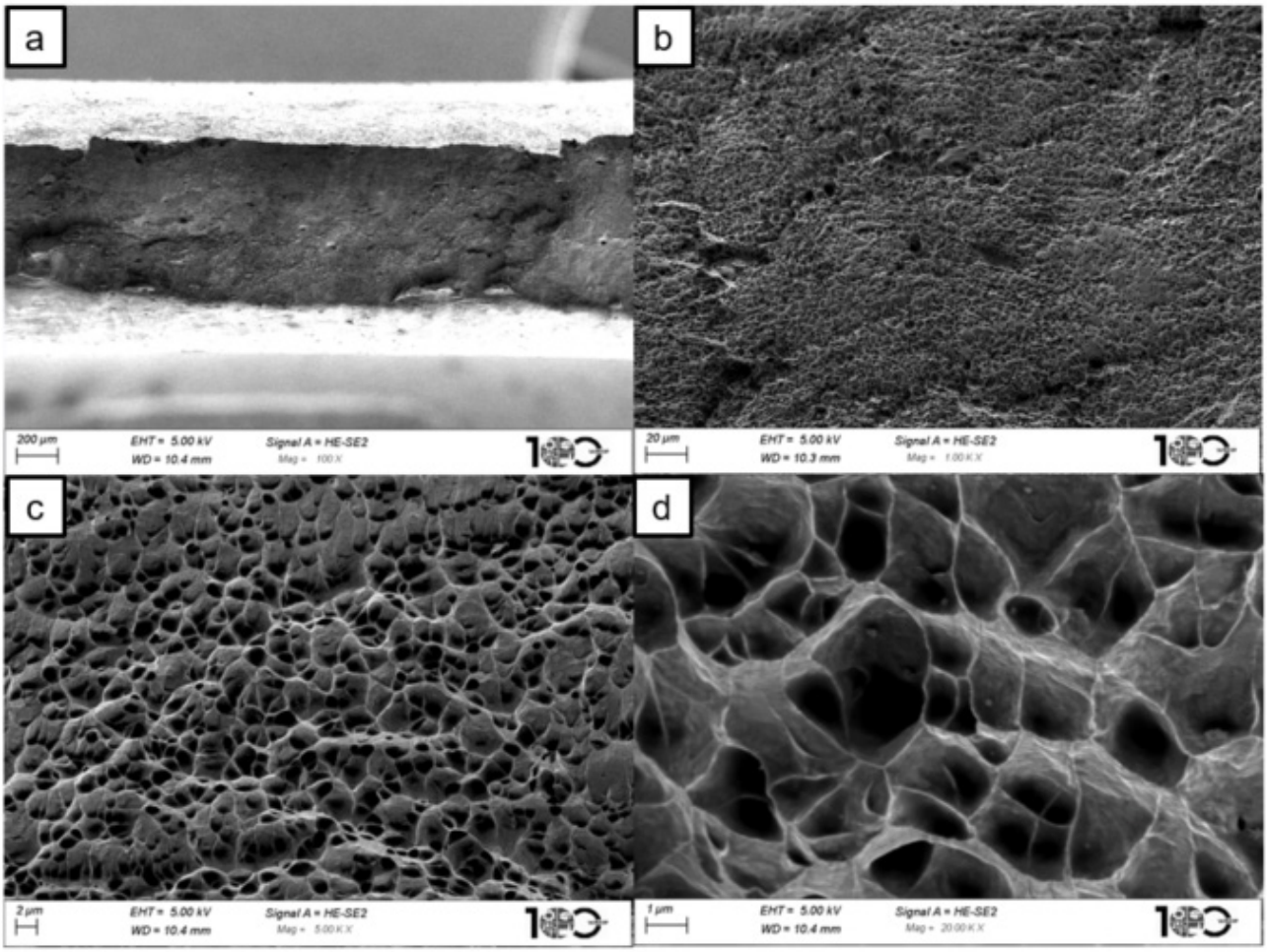

Fig. 11. Fractures formed during the tensile test observed on the side of steel 304L using various magnification values (SEM)

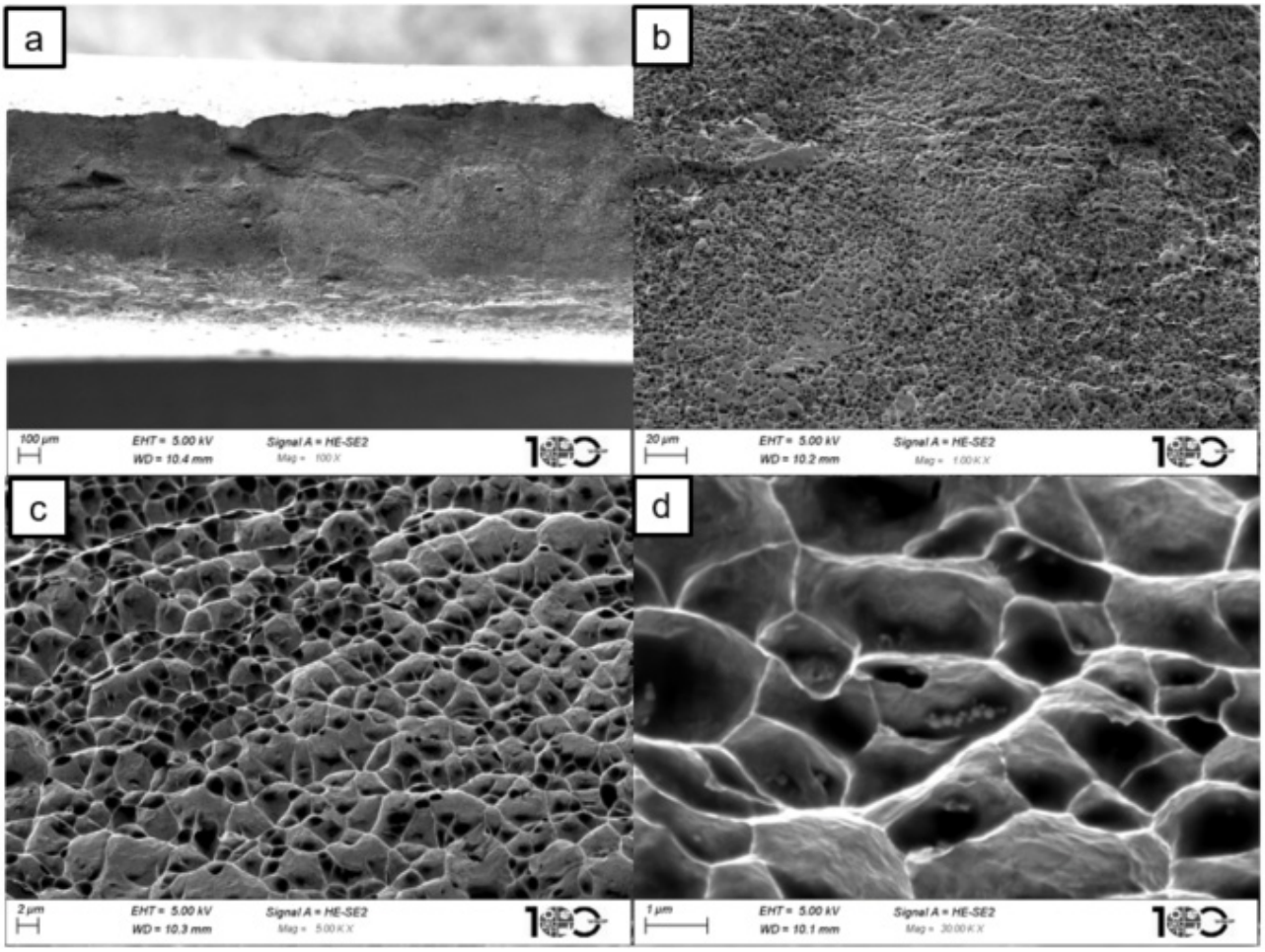

Fig. 12. Fractures formed during the tensile test observed on the side of steel 904L using various magnification values (SEM)

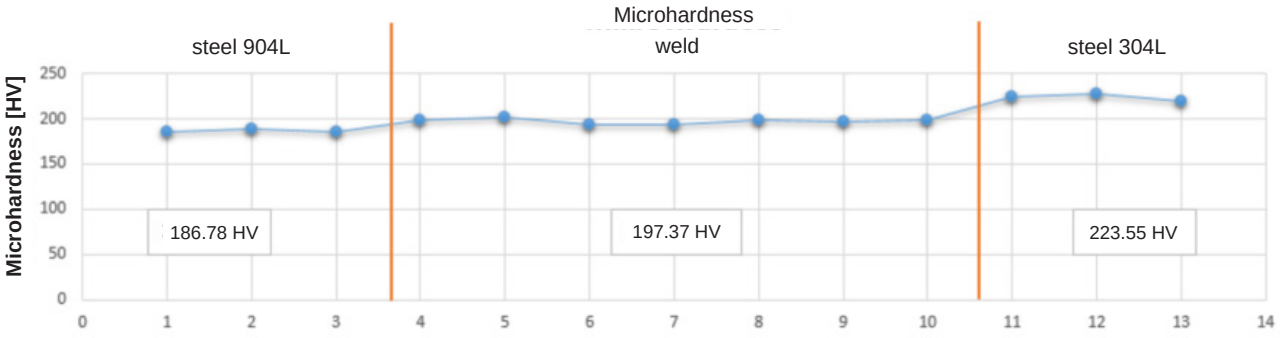

Fig. 13. Changes of microhardness across the welded joint /Microhardness; steel 904L; weld; steel 304L; Microhardness [HV]/

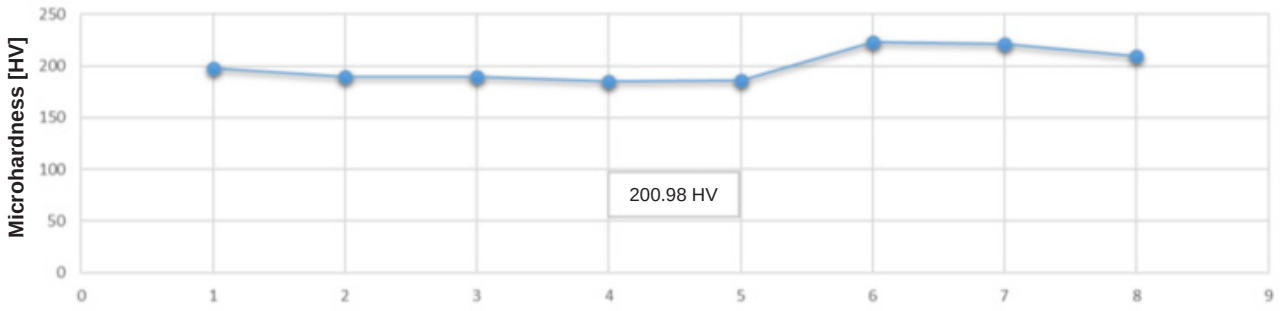

Fig. 14. Changes of microhardness across the welded joint

axis amounted to 201HV. The results obtained in the measurements of the weld hardness in both directions as well as the hardness values of both base materials justified the conclusion that the microstructure of the weld was homogenous, where the base materials constituting the former were mixed in an approximate ratio of 50/50.

Summary

Research works concerning increasingly advanced joints of materials contribute to the obtainment of more favourable results in each industrial sector. The search for new solutions enabling the reduction of manufacturing costs constitutes one of the most important directions of development in today's world. The tests performed within the study discussed in the article enabled the identification of the microstructure and mechanical properties facilitating a decision whether to implement or abandon the implementation of a new solution in the automotive industry.

Further research works concerning the above-presented area will include examinations of the welded joint cross-section following the static tensile test. The aim of the aforesaid tests will include the more detailed analysis of the course of crack-related phenomena taking place during the tensile test. Additional tests should involve the determination of the effect of laser beam welding parameters on the microstructure and properties of the welded joint as well as similar tests involving thinner and/or thicker sheets/plates.

The research work, performed in collaboration with PROGRESJA S.A. seated at ul. Żelazna 9, 40-851 Katowice, received research support of Międzynarodowe Centrum Mikroskopii Elektronowej dla Inżynierii Materiałowej /International Centre of Electron Microscopy for Materials Science (IC-EM), Akademia Górniczo-Hutnicza im. Stanisława Staszica w Krakowie (AGH University of Science and Technology in Kraków).

References

[1] Pilarczyk J. [ed.] et al.: Poradnik inżyniera, cz. 2. Spawalnictwo. Wydawnictwa Naukowo-Techniczne, Warszawa 2005.
[2] Klimpel A.: Spawanie, zgrzewanie i cięcie metali. Wydawnictwo Naukowo-Techniczne, Warszawa 1999.
[3] Maistro G.: Microstructural Characterization of Expanded Austenite in 304L and 904L Austenistic Stainless Steels. Chalmers University of Technology, Gothenburg, Sweden 2015.
[4] PN EN 10088-2:2014-12 Stale odporne na korozję – Część 2: Warunki techniczne dostawy blach cienkich/grubych i taśm ze stali nierdzewnych ogólnego przeznaczenia.
[5] PN EN ISO 4136 – Badania niszczące spawanych złączy metali – próba rozciągania próbek poprzecznych.